

LA-UR-12-24367

Approved for public release; distribution is unlimited.

Title: Ultrasonic signatures at the superconducting and the pseudogap phase boundaries in YBCO cuprates.

Author(s):
Shechter, Arkady
Migliori, Albert
Betts, Jonathan B.
Balakirev, Fedor F.
McDonald, Ross David
Riggs, Scott C.
Ramshaw, Brad
Liang, Ruixing
Hardy, Walter N.
Bonn, Doug A.

Intended for: arXiv



Disclaimer:

Los Alamos National Laboratory, an affirmative action/equal opportunity employer, is operated by the Los Alamos National Security, LLC for the National Nuclear Security Administration of the U.S. Department of Energy under contract DE-AC52-06NA25396. By approving this article, the publisher recognizes that the U.S. Government retains nonexclusive, royalty-free license to publish or reproduce the published form of this contribution, or to allow others to do so, for U.S. Government purposes.

Los Alamos National Laboratory requests that the publisher identify this article as work performed under the auspices of the U.S. Department of Energy. Los Alamos National Laboratory strongly supports academic freedom and a researcher's right to publish; as an institution, however, the Laboratory does not endorse the viewpoint of a publication or guarantee its technical correctness.

Ultrasonic signatures at the superconducting and the pseudogap phase boundaries in YBCO cuprates.

Arkady Shekhter,¹ Albert Migliori,¹ Jon B. Betts,¹ Fedor F. Balakirev,¹ Ross D. McDonald,¹ Scott C. Riggs,² Brad J. Ramshaw,³ Ruixing Liang,³ Walter N. Hardy,³ and Doug A. Bonn³

¹*Pulsed Field Facility, NHMFL, Los Alamos National Laboratory, Los Alamos, NM 87545*

²*Stanford Institute for Materials and Energy Sciences,*

SLAC National Accelerator Laboratory, Stanford CA

³*University of British Columbia, Vancouver, Canada*

(Dated: August 28, 2012)

A major issue in the understanding of cuprate superconductors is the nature of the metallic state from which high temperature superconductivity emerges. Central to this issue is the pseudogap region of the doping-temperature phase diagram that extends from room temperature to the superconducting transition. Although polarized neutron scattering studies hint at magnetic order associated with the pseudogap, there is no clear thermodynamic evidence for a phase boundary. Such evidence has a straightforward physical interpretation, however, it is difficult to obtain over a temperature range wide enough to encompass both the pseudogap and superconducting phases. We address this by measuring the elastic response of detwinned single crystals, an underdoped $\text{YBCO}_{6.60}$ with superconducting transition at $T_c = 61.6\text{K}$ and a slightly overdoped $\text{YBCO}_{6.98}$ with $T_c = 88.0\text{K}$. We observe a discontinuity in the elastic moduli across the superconducting transition. Its magnitude requires that pair formation is coincident with superconducting coherence (the onset of the Meissner effect). For both crystals the elastic response reveals a phase transition at the pseudogap boundary. In slightly overdoped YBCO that transition is 20K below T_c , extending the pseudogap phase boundary inside the superconducting dome. This supports a description of the metallic state in cuprates where a pseudogap phase boundary evolves into a quantum critical point masked by the superconducting dome.

Introduction. Resonant ultrasound spectroscopy (RUS) measures the frequencies f_n of the mechanical resonances of a macroscopic specimen.^{1,2} Using the redundant information contained in the frequency shifts $\Delta f_n(T)$, which in the measurements reported here are proportional to linear combinations of the small changes in elastic moduli, RUS can measure the temperature evolution of elastic moduli $\Delta c_{ij}(T)$ with sensitivity exceeding 1 part per million. Like heat capacity, thermal expansion, and a very few other thermodynamic susceptibilities, elastic moduli are sensitive to all changes in the thermodynamic state of a system. If the pseudogap is a distinct phase like the superconducting transition, it must be accompanied by a thermodynamic signature evident in the elastic moduli. Unlike (scalar)

heat capacity, elastic moduli have several components, thus contain information about the symmetry of a phase transformation. The universal behavior observed in the metallic state at higher temperatures^{3–7} does not extend below the pseudogap phase boundary, T^* . Evidence for time reversal and inversion symmetry breaking^{8–10} in the pseudogap phase suggests a continuous (second order) transition as developed in Ref. 11.

A strength of ultrasonic measurements is that the thermodynamic information is accompanied by transport information contained in the ultrasonic attenuation¹², which unlike electrical conductivity is not hidden by superconductivity. For resonance methods, attenuation is measured by the inverse quality factor, proportional to the width of the resonance. Such measurements on millimeter-sized detwinned YBCO crystals face a range of experimental challenges. These include vibration isolation over a broad temperature range, stable specimen positioning without adhesives, use of minimal ultrasonic power while maintaining required signal-to-noise ratio, and temperature control under conditions where thermal contact to the crystal is weak (Figure 1; SI contains experimental details).

Ultrasound and high temperature superconductivity in cuprates. Elastic moduli, second derivatives of the free energy, must change discontinuously (jump) across a second order phase transition, softening upon cooling into a symmetry-broken phase. The softening originates in the difference between the “fast” and “slow” elastic response in the symmetry-broken phase, $-\Delta c_{ij} = c_{ij}^\eta - c_{ij}^\phi$. Analogous to adiabatic and isothermal measurements, here the term “fast” moduli, c_{ij}^η , corresponds to the response at fixed order parameter η , whereas “slow” moduli, c_{ij}^ϕ , correspond to moduli where the order parameter is at equilibrium, *i.e.* $\phi = dF/d\eta$, the order parameter restoring force is zero. The order parameter has a finite, temperature dependent relaxation time $\tau(T)$ which lengthens close to a transition (critical slowing down)¹⁶. This means that in a measurement at finite frequency, ω , the softening extends over a finite temperature range in which the system crosses from $1/\tau(T) \ll \omega$ to $1/\tau(T) \gg \omega$. Causality requires that the dynamic origin of the broadening of the discontinuity in the frequency shift is accompanied by increased attenuation over the same range of

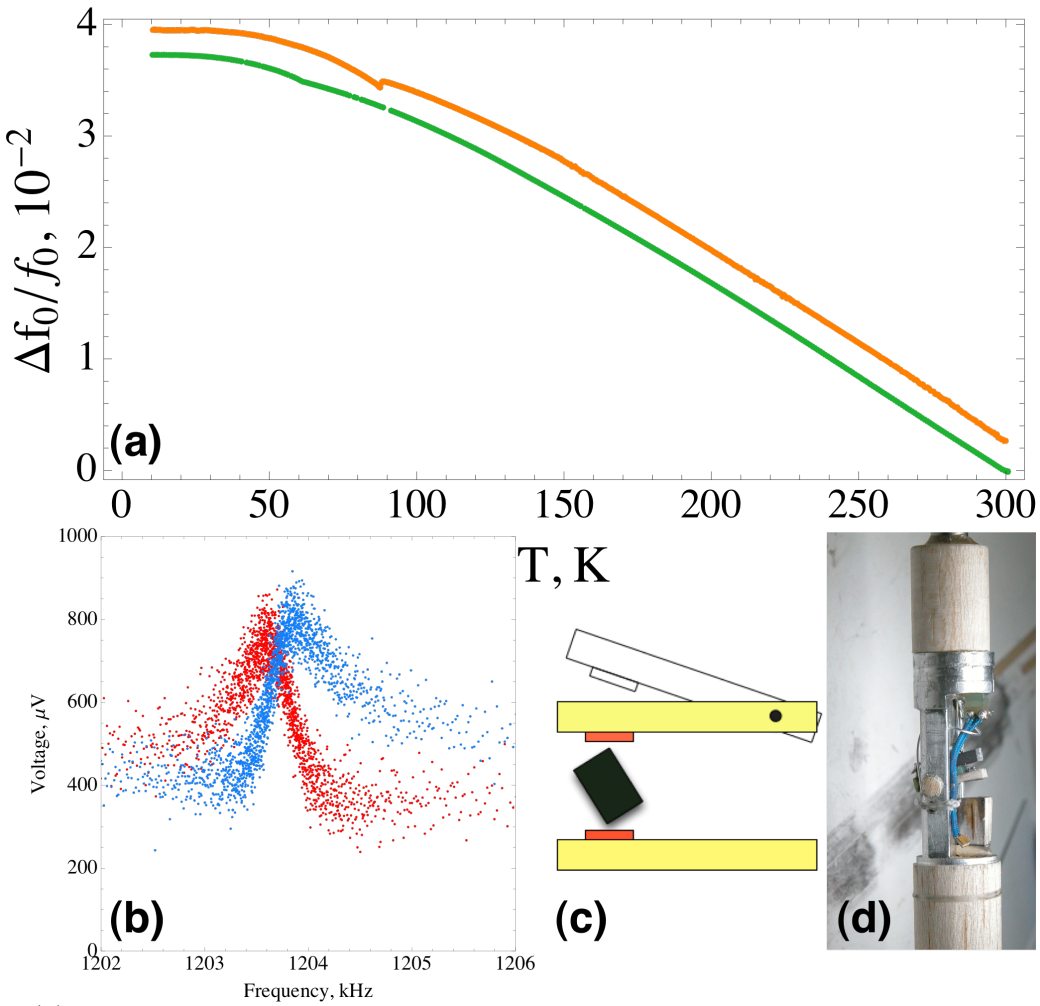


FIG. 1. (a) Mechanical resonance frequency shift versus temperature for underdoped YBCO_{6.60}, $T_c = 61.6K$ (hole doping $p = 0.108 \pm 0.005^{13}$), green, and slightly overdoped YBCO_{6.98} ($T_c = 88K$, hole doping $p = 0.188$), orange. Crystals are approximately $200\mu m$ thick, and one mm square. The two curves are offset vertically for clarity. In YBCO (as in most crystals) the largest component (up to 5%) of the temperature dependence of elastic moduli upon cooling from room temperature to zero is associated with the anharmonicity of the lattice¹⁴. The anharmonicity-driven frequency shift is smooth and monotonic¹⁵. (b) a typical resonance taken with the low acoustic power required, in-phase (red), quadrature (blue) components. (c) transducer-sample geometry. (d) balsa-wood probe used in the measurement.

temperature (Kramers-Kronig in SI).

Compressional elastic moduli (crystallographic scalars¹⁷) enter linearly in the free energy and therefore can change discontinuously at a phase transition. Volume preserving moduli (shear) can be discontinuous only in their derivatives (break in slope). The magnitude of the

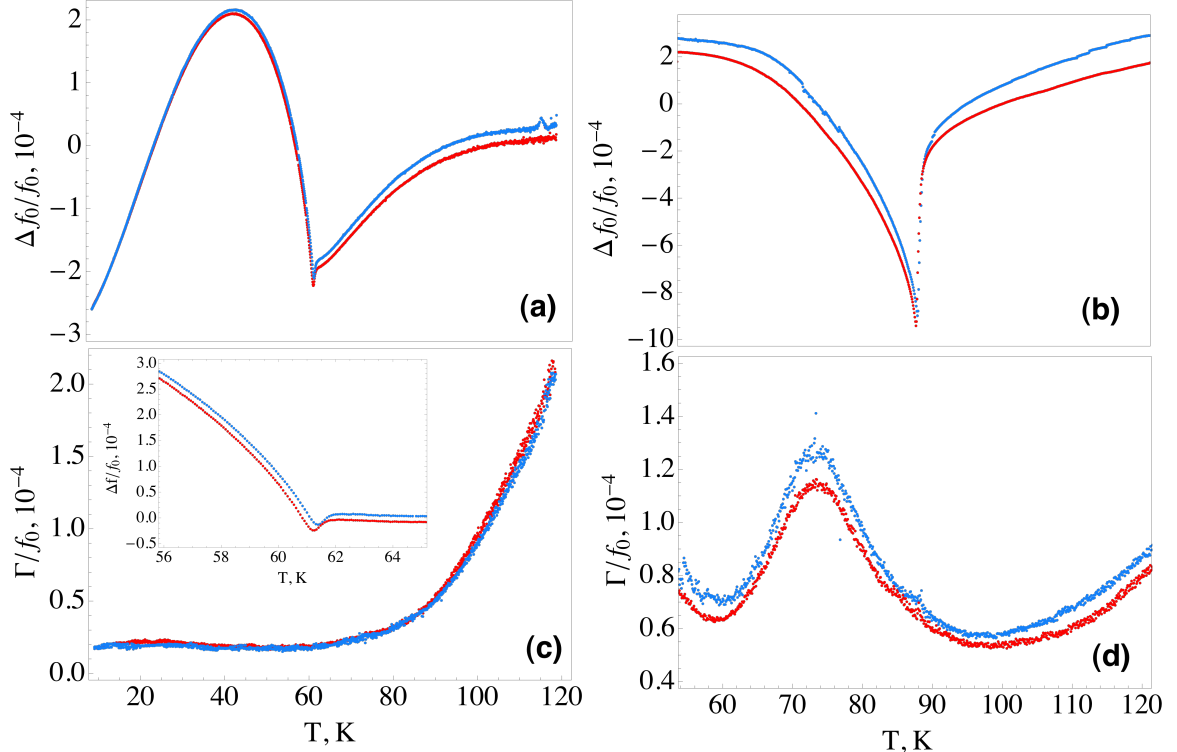


FIG. 2. (a,c) Resonance frequency with anharmonic background subtracted (a) and attenuation (c) across the superconducting transition in the $\text{YBCO}_{6.60}$ crystal. Inset in (c) shows frequency shift across T_c . 50mK intervals were used on cooling (blue), 70mK on heating (red) in a continuous temperature-controlled linear-in-time temperature sweep (SI for details). A small horizontal offset between heating and cooling, $\sim 0.2K$, clearly visible at the superconducting transition, is caused by imperfect thermal contact between thermometer and crystal. The origin of the vertical offset is unclear but not surprising for such high resolution scans. (b,d) Resonance frequency shift with anharmonic background subtracted (b) and attenuation (d) in 90mK steps for the $\text{YBCO}_{6.98}$ crystal. The maximum in attenuation in the $\text{YBCO}_{6.98}$ crystal is not associated with the superconducting transition as will be discussed in the text. Note that changes in elastic moduli clearly associated with the superconducting transition extend as far as 50K above and below T_c .

(dimensionless) step discontinuity, required at a the superconducting transition, is, within a factor of order unity, equal to $(T_c/T_F)^2$, where T_F is a degeneracy temperature of the metallic state from which superconductivity emerges - for conventional metals the Fermi temperature. (SI contains details)

The temperature dependence of a given resonance f_n depends on changes in several elastic moduli c_{ij} weighted with geometric factors α_{ij}^n , of order unity, which depend on crystal shape and the mode of vibration, $\Delta f_n(T)/f_n = \sum_{ij} \alpha_{ij}^n (\Delta c_{ij}(T)/c_{ij})$. The lowest resonant frequencies are typically determined by shear elastic moduli alone, which in YBCO are about 1/3 that of compressional moduli¹⁸. The crystal shape determines the particular mix of moduli for each resonance.¹ The largest frequency shifts across the superconducting transition can be used to infer a lower bound on the thermodynamic effects at the phase transition. In underdoped YBCO_{6.60} we measured a shift $\Delta f/f \approx 10^{-4}$, and for slightly overdoped YBCO, $\Delta f/f$ is an order of magnitude larger (Figure 2). Because there is no significant attenuation increase at the superconducting transition, the transition width, $\Delta T_c = 0.5K$, is not associated with dynamics^{19,20} and therefore must be caused by small variations in hole doping over the volume of the crystal. With $T_F \sim 5000K$ and $T_c/T_F \sim 10^{-2}$, the magnitude of the observed elastic discontinuity at both dopings is consistent with the entire thermodynamic signature of superconductivity occurring within 0.5K of the transition.

The phase transition at the pseudogap phase boundary. On cooling, the resonance frequency shift in YBCO_{6.60} reveals a break in slope at $T^* = 245K$, a standard marker for a phase transition, Figure 3. This temperature corresponds well with the onset temperature of magnetic order reported in YBCO specimens of similar composition.⁹ For phase transitions of the class indicated by neutron diffraction^{9,10} there is no requirement for a step discontinuity.²¹ The pseudogap temperature, T^* , varies much more rapidly with oxygen composition than the superconducting transition temperature – near oxygen doping $x = 6.60$, $dT^*(p)/dp$ is about 10 times larger than $dT_c(p)/dp$, Figure 3(d). This is consistent with the observed $\Delta T^* = 5K$ width of the pseudogap transition, about 10 times that of the superconducting transition, $(dT^*/dT_c)\Delta T_c$.

The phase transition at $T^* = 245K$ is accompanied by a strong increase in attenuation above T^* . This ultrasonic attenuation¹² is caused by the slowing down of fluctuations, reaching a

maximum when the measurement frequency matches the characteristic timescale, $\omega\tau(T) = 1$ (details in SI). Frequently¹⁶ attenuation reaches a maximum on the symmetry-broken side of a transition and spans a temperature range equal to the transition width. However, for YBCO (Figure 3) the attenuation maximum occurs at a temperature higher than the pseudogap transition, and spans a temperature range wider than the width of the transition. On heating, the pseudogap transition is broader than on cooling. The transition exhibits approximately 10K hysteresis (details in SI). The small discontinuities in frequency observed upon cooling in the pseudogap phase (Figure 3(a)) do not occur in similar sized well behaved metals in the same apparatus. Such variations are reminiscent of the response of domains, especially in that they depend on cooling rate and history and are absent on heating. It is possible that although the crystals are detwinned, a very small number of crystallographic twin boundaries could be present.

For the slightly overdoped crystal, YBCO_{6.98}, the break in slope occurs at 67K. Extrapolating $T^*(p)$ from measurements in underdoped cuprates (Figure 3(d)), we conclude that this phase transition is the pseudogap phase boundary, extending T^* 20K below the superconducting transition near optimal doping. This extends the doping range over which magnetic order exists to the vicinity of optimal doping. The width of the attenuation maximum associated with the pseudogap appears to scale with T^* . The resonances exhibit a strong (up to hundred-fold) increase in ultrasonic attenuation over a narrower temperature range (60K and 80K) than in the underdoped crystal. This reveals a correlation between the measurement frequency and the temperature of the attenuation maximum (Figure 4). Interpreting this frequency dependence as originating from $\omega\tau(T) = 1$ reveals the divergence of $\tau(T)$ as the pseudogap phase transition is approached. In Figure 4(e) the extrapolated value of $1/\tau(T)$ vanishes close to 65K. Like the underdoped specimen, the strong increase in ultrasonic attenuation is observed above the pseudogap phase boundary. Note that the frequency shift is upward on cooling to the symmetry broken phase (SI for more discussion).

The resonance measurements presented here provide quantitative bounds on the dis-

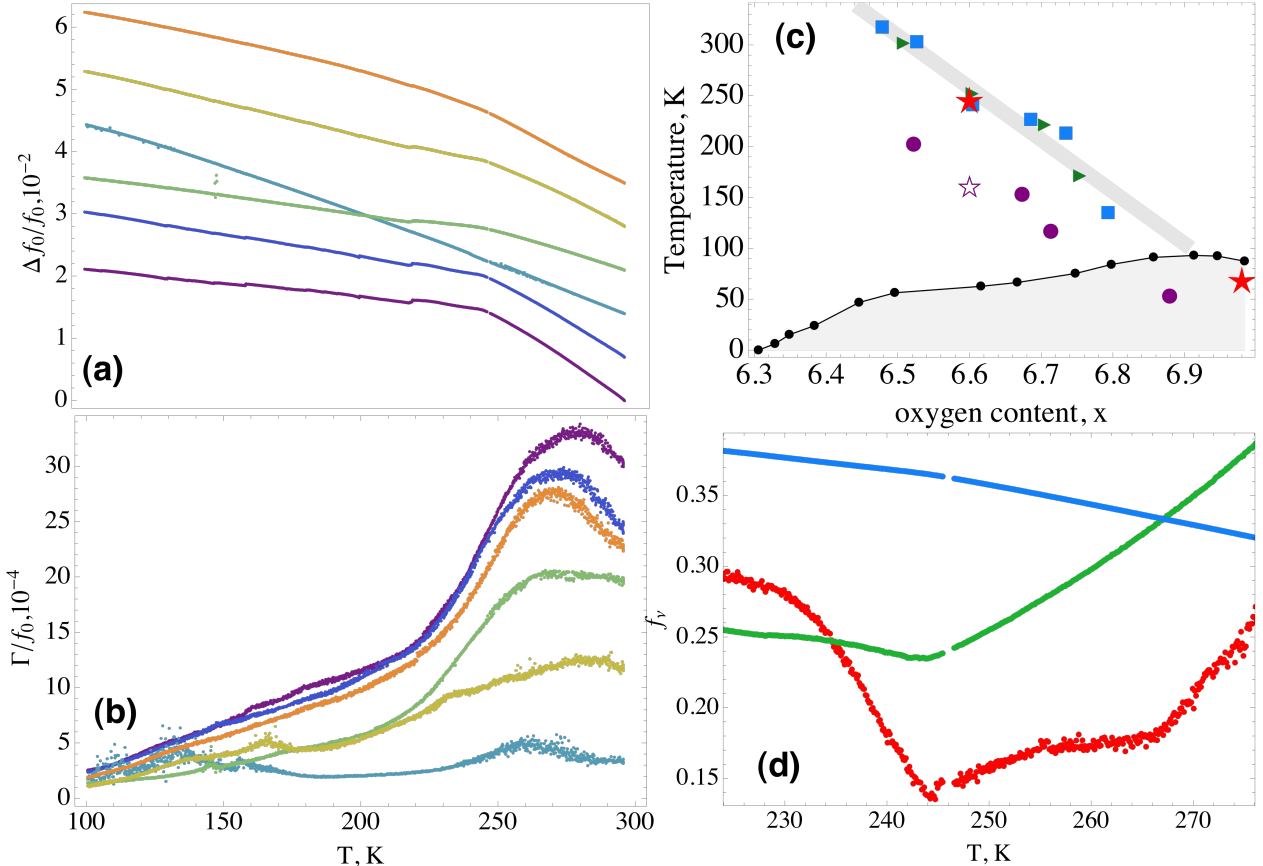


FIG. 3. Resonance frequency shift (a) and linewidth (b) vs temperature in $\text{YBCO}_{6.60}$ for several modes. For clarity the frequency shift curves are offset vertically. A clear increase in ultrasonic attenuation is observed close to the onset temperature of Kerr rotation²². The many different temperature dependences in (a) can be decomposed into three linearly independent components (d) (SI has details). It is required that there be no more than 6 such components (tetragonal symmetry) and, likely, fewer because some of the six independent elastic moduli will have similar temperature dependences. At least one should not show anything at T^* , as is observed. (c) Phase diagram of hole-doped cuprates. Neutron diffraction⁹ (blue squares), magnetic susceptibility²³ (triangles), Kerr rotation²² (circles), Resonant Ultrasound (stars). The error in determining T^* from neutron diffraction is about 50K. The error in determining T^* from RUS measurements is the apparent width of the transition, not the intrinsic precision of RUS (frequency errors are negligible, temperature errors are less than 20mK).

continuity in the elastic moduli across the superconducting transitions, and rule against the thermodynamics of pairing occurring at temperatures above T_c in both underdoped and slightly overdoped YBCO. These observations also support a description of the metallic state and high temperature superconductivity in cuprates where a pseudogap phase bound-

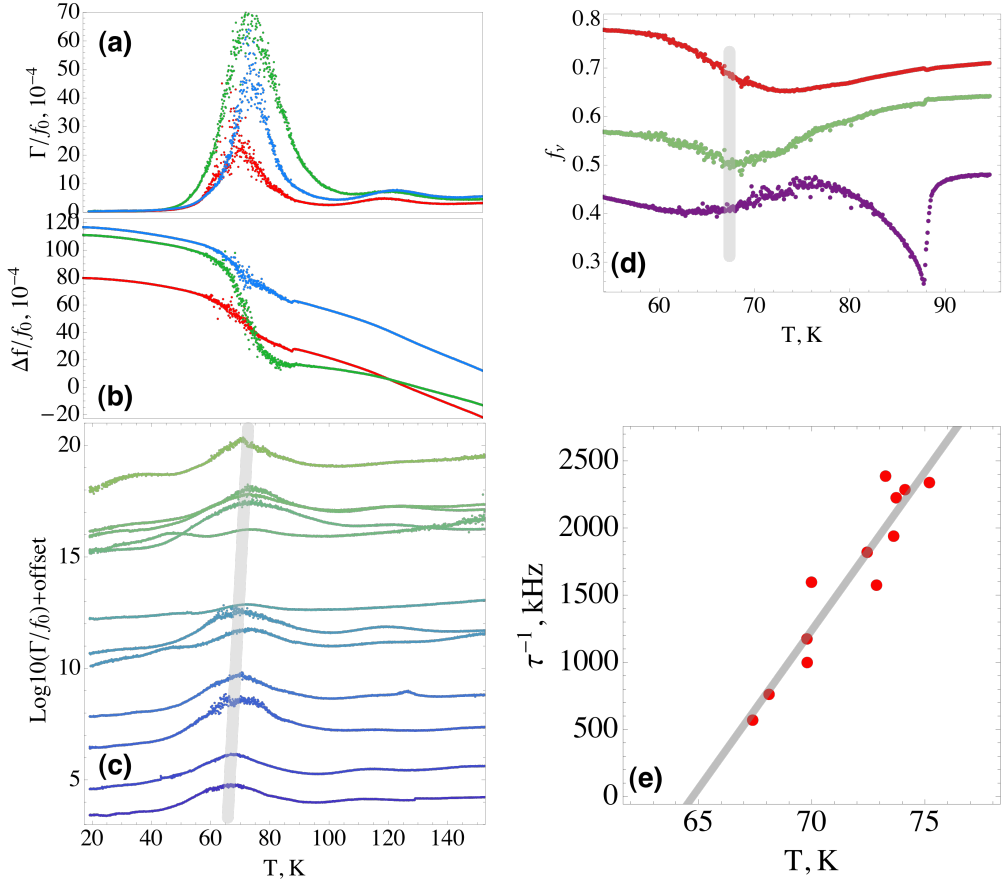


FIG. 4. RUS measurements across the pseudogap phase boundary in slightly overdoped YBCO. Ultrasonic attenuation (a) and resonance shift vs temperature (b) for three resonance peaks showing strong (up to hundred-fold) increase in ultrasonic attenuation. There is a weak maximum near 120K that is frequency dependent. (b) curves offset vertically. (c) logarithm of resonance width for several modes, with vertical offset. Gray: evolution of the attenuation maximum with mode frequency. (d) independent linear components of the temperature dependence of several resonance peaks. The green curve shows a break in slope at $T^*=67\text{K}$, the red curve shows only a smooth background also present in green and purple, and the purple curve shows the superconducting discontinuity. (e) from the plot of attenuation versus temperature (c), we extract the temperature of the attenuation maximum, and the frequency at which this occurs (noting that $\omega\tau(T) = 1$ at that frequency) and plot $1/\tau(T)$ versus that temperature (e).

ary evolves into a quantum critical point masked by superconductivity.

Acknowledgements We thank Martin Greven, Chandra Varma and Inna Vishik for critical reading of the manuscript. We thank James Analytis, Neil Harrison, and Guichuan Yu for

informative discussions. Work at Los Alamos National Laboratory (LANL) was supported by NSF-DMR-0654118, DOE, and the State of Florida. LANL is operated by LANS LLC.

- ¹ A. Migliori, J. M. Sarrao, *Resonant Ultrasound Spectroscopy*, Wiley-Interscience (1997).
- ² A. Migliori, J. D. Maynard, *Review of Scientific Instruments* **76**, 1 (2005).
- ³ P. W. Anderson, *Science* **256**, 1526 (1992).
- ⁴ C. M. Varma, P. B. Littlewood, S. Schmitt-Rink, E. Abrahams, and A. Ruckenstein, *Phys. Rev. Lett.* **63**, 1996 (1989).
- ⁵ T. Kondo, Y. Hamaya, A. D. Palczewski, T. Takeuchi, J. S. Wen, Z. J. Xu, G. Gu, J. Schmalian, and A. Kaminski, *Nature Physics* **7**, 21 (2011).
- ⁶ M. Quervitch, and A. T. Fiory, *Phys. Rev. Lett.* **59**, 1337 (1987).
- ⁷ J. L. Tallon, and J. W. Loram, *Physica* **C349**, 53 (2001).
- ⁸ A. Kaminski, S. Rosenkranz, H. M. Fretwell, J. C. Campuzano, Z. Li, H. Raffy, W. G. Cullen, H. You, C. G. Olson, C. M. Varma, and H. Höchst, *Nature* **416**, 610 (2002).
- ⁹ B. Fauqué, Y. Sidis, V. Hinkov, S. Pailhès, C. T. Lin, X. Chaud, and P. Bourges, *Phys. Rev. Lett.* **96**, 197001 (2006).
- ¹⁰ Y. Li, V. Baledent, N. Barisic, P. Bourges, Y. Cho, B. Fauque, Y. Sidis, G. Yu, X. Zhao, and M. Greven, *Nature* **455**, 372 (2008).
- ¹¹ C. M. Varma, *Phys. Rev. B* **55**, 14554 (1997).
- ¹² A. B. Bhatia, *Ultrasonic Absorption*, Oxford, Clarendon Press (1967).
- ¹³ R. Liang, W. Hardy, D. Bonn, *Phys. Rev. B* **73**, 180505 (2006).
- ¹⁴ Y. Varshni, *Phys. Rev. B* **2**, 3952 (1970).
- ¹⁵ A. Migliori, C. Pantea, H. Ledbetter, I. Stroe, J. B. Betts, J. N. Mitchell, M. Ramos, F. Freibert, D. Dooley, S. Harrington, and C. H. Mielke, *J. Acoust. Soc. Am.* **122**, 4 (2007).
- ¹⁶ L. D. Landau, and I. M. Khalatnikov, *Dokl. Akad. Nauk SSSR* **96**, 469 (1954) [English translation: in *Collected papers of L. D. Landau*, edited by D. ter Haar, Pergamon, London (1965)].
- ¹⁷ R. R. Birss, *Symmetry and Magnetism*, (Wiley-Interscience Inc., New York, 1964).

¹⁸ *Phys. Rev. B* **47**, 6154 (1993).

¹⁹ A. Junod, A. Erb, and C. Renner, *Physica C* **318**, 333 (1999).

²⁰ V. Pasler et.al., *Phys. Rev. Lett.* **81**, 1094 (1998).

²¹ M. S. Grønsletth, T. B. Nilssen, E. K. Dahl, E. B. Stiansen, C. M. Varma, and A. Sudbo, *Phys. Rev. B* **79**, 094506 (2009).

²² J. Xia, E. Schemm, G. Deutscher, S. A. Kivelson, D. A. Bonn, W. N. Hardy, R. Liang, W. Siemons, G. Koster, M. M. Fejer, and A. Kapitulnik, *Phys. Rev. Lett.* **100**, 127002 (2008).

²³ B. Leridon, P. Monod, and D. Colson, *Europhys. Lett.* **87**, 17011 (2009).